



Predictive gamma passing rate of 3D array detector-based VMAT QA via deep learning combining dose distribution and accumulated dose uncertainty potential distribution

Takaaki Matsuura,^{1,2*} Daisuke Kawahara,² Akito Saito,³ Eiji Shiba,^{2,4} Kiyoshi Yamada,¹ Shuichi Ozawa,^{1,2} Yasushi Nagata^{1,2}

¹ Hiroshima High-Precision Radiotherapy Cancer Center, Hiroshima, Japan

² Department of Radiation Oncology, Graduate School of Biomedical & Health Science, Hiroshima University, Hiroshima, Japan

³ Department of Radiation Oncology, Hiroshima University Hospital, Hiroshima, Japan

⁴ Department of Radiation Oncology, Hospital of the University of Occupational and Environmental Health, Fukuoka, Japan



AIM

In the intensity-modulated radiation therapy (IMRT) and volumetric modulated arc radiotherapy (VMAT), several guidelines recommend performing measurement-based verification as patient-specific quality assurance (QA) before clinical treatment.¹⁾

Recent studies proposed predicting models of the gamma passing rate (GPR) for improving the efficiency of the patient-specific quality assurance (QA) processes. For example, a deep learning-based predicting method using 2D dose distribution by gafchromic film precisely predicted the GPR.²⁾ On the other hand, recent IMRT QA has been performed with the 3D measurement in actual clinical practice. Moreover, our group proposed the dose uncertainty potential (DUP) based predicting method was extended to three-dimensional (3D) measurement, and the accumulated DUP is closely related to GPR.^{3,4)}

The current study aims to develop a deep convolution neural network (DCNN) model for predicting GPR of 3D array detector with 3D dose distribution and accumulated DUP distribution.

MATERIALS AND METHODS

135 prostate VMAT plans using 10 MV X-ray of the TrueBeam with dual-arc created in the Eclipse treatment planning system (TPS) were retrospectively collected. These plans were performed dose distribution QA using the ArcCHECK dosimetry system. The gamma analysis was performed for four tolerances (3%/3 mm, 3%/2 mm, 2%/3 mm, and 2%/2 mm) with a 10% dose threshold, absolute dose mode, and global normalization. 110 cases were used for training and validation, and the rest 25 cases were used for the test.

The dose distribution and the DUP distribution on the cylindrical detector plane of these verification plans were generated from DICOM RT-Plan and Dose exported from the treatment planning system (Eclipse) by in-house software (python). The DUP distribution is accumulated field edges weighted by a segmental monitor unit followed by Gaussian folding. These two distributions were used as input data for the DCNN. As shown in Fig. 1, the DCNN with the dose distribution only is Model I, and with two distributions is Model II. The measured GPR values were used as output data for the DCNN.

Our DCNNs were trained for 200 epochs, and the network was optimized using Adam. The drop rates of the dropout layer were set to 0.25. The architecture of the DCNN was implemented in a central process unit using the Keras framework and TensorFlow as the backend. Five-fold cross-validation was applied to verify the predicting performance. The prediction of the GPR was repeated five fractions, and the average values of these GPR were defined as the final prediction results for test cases. The difference between the measured and predicted GPR values was evaluated for Model I and Model II.

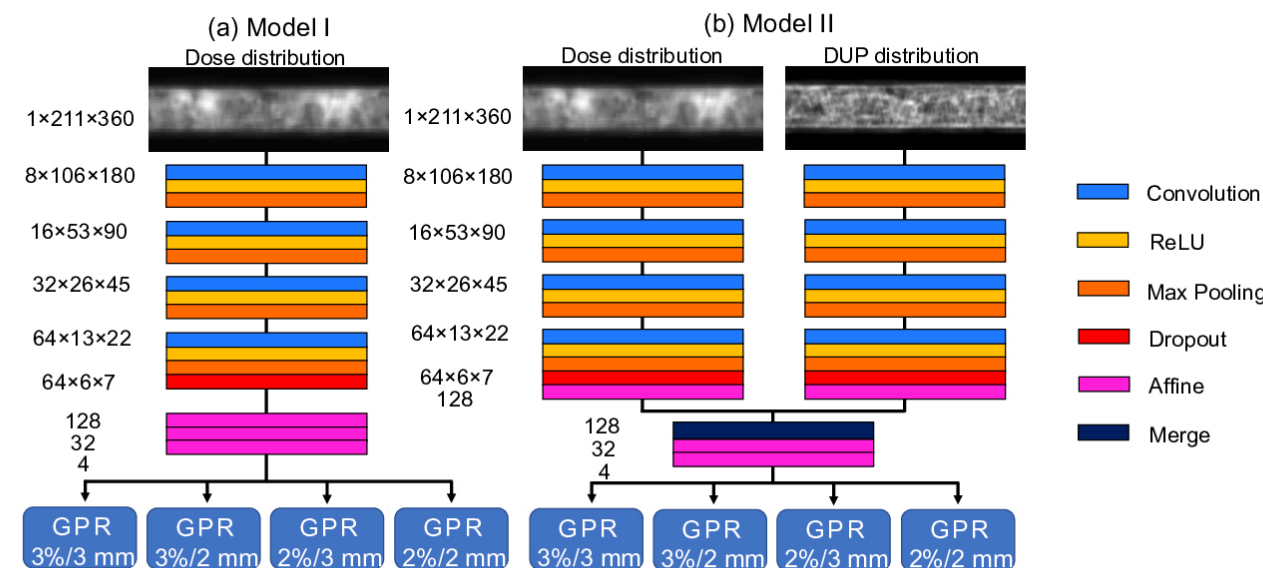


Fig.1: Schematic diagrams of the DCNN architecture with (a) the dose distribution (Model I) and (b) the dose + DUP distribution (Model II).

RESULTS

Figure 2 shows the correlations of measured GPR with predicted GPR in Model I (dose distribution) and Model II (dose distribution + DUP distribution) for four tolerances. Both prediction models had high linearity of measured GPR and predicted GPR.

In the Model I, the probabilities of the cases with prediction error within 3% were 80%, 52%, 72%, and 64% for 3%/3-mm, 3%/2-mm, 2%/3-mm, and 2%/2-mm tolerances, respectively. In the Model II, the probabilities of the cases with prediction error within 3% were 84%, 68%, 76%, and 60% for 3%/3-mm, 3%/2-mm, 2%/3-mm, and 2%/2-mm tolerances, respectively.

Table 1 summarizes the mean value and SD of predicted GPR, measured GPR, MAE, RMSE, and CC for tolerances in Model I and Model II. The accuracy of predicted GPR was improved by adding the DUP distribution to input data for the DCNN.

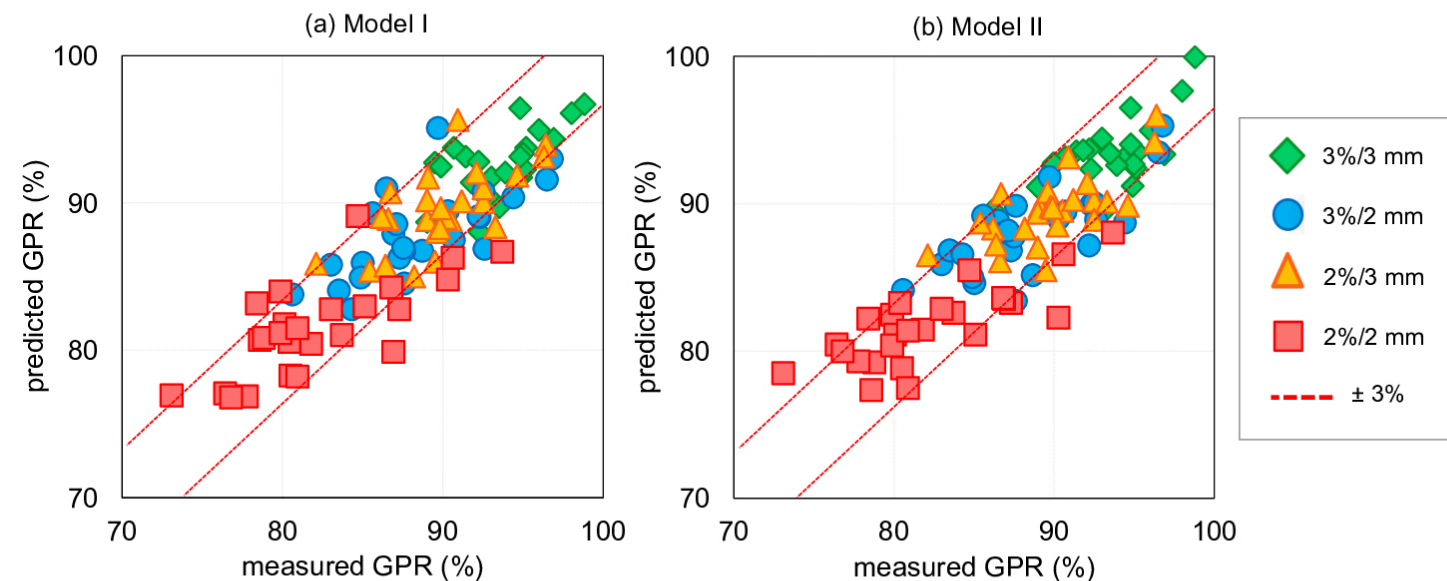


Fig. 2: The correlation of measured GPR with predicted GPR in (a) Model I and (b) Model II for four tolerances.

Table 1: Summary of predicted and measured GPR values (%) and evaluation items for each tolerances.

		Model I						Model II			
		Mean	SD	Mean ± SD	MAE	RMSE	CC*	Mean ± SD	MAE	RMSE	CC*
3%/3 mm	measured	93.2	3.0	-0.9 ± 2.2	2.1	2.4	0.67	0.1 ± 2.1	1.8	2.1	0.69
	predicted	92.4	2.4								
3%/2 mm	measured	88.6	4.2	-0.7 ± 2.9	2.5	3.0	0.70	-0.4 ± 2.8	2.4	2.8	0.74
	predicted	87.9	3.0								
2%/3 mm	measured	89.9	3.4	-0.4 ± 2.5	2.2	2.6	0.66	-0.3 ± 2.3	1.9	2.4	0.71
	predicted	89.5	2.7								
2%/2 mm	measured	82.3	4.9	-0.7 ± 3.3	2.8	3.4	0.73	-0.5 ± 3.2	2.6	3.3	0.78
	predicted	81.5	3.2								

SD: standard deviation; MAE: mean absolute error; RMSE: root mean squared error; CC: correlation coefficient. * $p < 0.01$

DISCUSSION / CONCLUSION

The features of the dose distribution on the cylindrical detector plane are considered to have a direct relationship with measured GPR. The cylindrical dose distribution retains features of the treatment plan since the entrance, and exit dose for each control point is accumulated at each detector element.

By adding the DUP distribution to input data of DCNN, the accuracy of predicted GPR was improved. It was indicated that the accumulated DUP distribution obtained the feature related to the complexity of the treatment plan that the dose distribution cannot obtain.

Limitation

The treatment site for the prediction was limited to the prostate in this study. It is necessary to broaden the target of predicted treatment sites to apply our method to clinical practice and to simplify the QA process in many treatment cases.

Conclusion

The DCNN with the dose and DUP distributions on the cylindrical detector element plane could predict the GPR of 3D detector array-based VMAT QA value with high accuracy. These findings could potentially help to omit the patient-specific QA measurements.

REFERENCES

- Ezzell GA, Burmeister JW, Dogan N, et al. IMRT commissioning: multiple institution planning and dosimetry comparisons, a report from AAPM Task Group 119. Med Phys. 2009;36:5359–5373.
- Tomori S, Kadoya N, Takayama Y, et al. A deep learning-based prediction model for gamma evaluation in patient-specific quality assurance. Med Phys. 2018;45:4055–4065.
- Shiba E, Saito A, Furumi M, et al. Predictive gamma passing rate by dose uncertainty potential accumulation model. Med Phys. 2019;46:999–1005.
- Shiba E, Saito A, Furumi M, et al. Predictive gamma passing rate for three-dimensional dose verification with finite detector elements via improved dose uncertainty potential accumulation. Med Phys. 2020;47:1349–1356.

Conflict of Interest Notification: none

CONTACT INFORMATION

EMAIL: matsuura@hiprac.jp